Variability of water mass interleaving off N.W. Africa

by E. D. Barton[1] and P. Hughes[1]

ABSTRACT

Water mass interleaving observed over the N.W. African continental slope during Upwelling 75 has been investigated. A water mass census demonstrated that the most common temperature-salinity characteristics over the slope at 23N lay between those of the North and South Atlantic Central Water masses. Filtering of vertical profiles of temperature, salinity and sigma-T was used to separate out the medium scale structure (vertical wavelengths between 4 and 80 m). Standard deviations of the medium scale profiles, used as an index of the intensity of interleaving, indicated a persistent maximum of interleaving 70 km seaward of the continental shelf edge. At any point the temperature and salinity structures were highly correlated and density compensating.

A water mass analysis, based on the assumption of isopycnal mixing, confirmed that the most intense interleaving coincided with a boundary or weak front between the two central water masses. Further hydrographic observations on sections near 25° 30′ N and 21° 30′ N and current measurements at five sites showed that the interleaving occurred at the offshore limit of a tongue of SACW which was being advected northward along the inner continental slope. Offshore, the NACW was associated with the southwestward drift of the Canary Current while currents in the region of most intense interleaving were highly variable in direction, suggestive of eddying and meandering associated with interleaving across the front. Inshore of the tongue of SACW, the flow on the continental shelf was strongly equatorward.

Time series observations of temperature and salinity from sensors on the moorings in the interleaving zone indicated that little variation in sigma-T occurred despite the great hydrographic variability, supporting the idea that mixing was mainly lateral. At the moorings on the inner slope changes in sigma-T were associated with variability of temperature and salinity, and indicated that vertical mixing and advection might be important. The space and time scales of the interleaving were estimated to be approximately: 25-30 m vertically, 20-70 km parallel to the front, <10 km across the front, and 2-7 days. Preliminary estimates of the cross-frontal heat fluxes, calculated from the hydrographic data and from the time series records of current and temperature, were found to have values of approximately 1 C cm s^{-1}.

1. Introduction

The waters near 23N off N.W. Africa are characterized by the interaction between the North and South Atlantic Central Water masses. To the north NACW is dominant, to the South SACW predominates but in the upper 500 m at latitudes

1. Department of Oceanography, University of Liverpool, P.O. Box 147, Liverpool, United Kingdom, L69 3BX.

near Cap Blanc a boundary zone or large scale front is present between these two water masses. In the frontal zone, water mass properties vary over the whole range of possible combinations of NACW and SACW. The water column is composed of numerous interleaved layers of varied temperature-salinity properties. The meridional extent of the boundary zone is apparently limited to a few degrees of latitude near the coast (Hughes and Barton, 1974; Fraga and Manriquez, 1975). Although the front between NACW and SACW has been shown to extend across the Atlantic (Sverdrup *et al.*, 1942), little is known of its detailed structure. The interleaving has been of incidental interest in studies of upwelling on the N.W. African continental shelf because it represents an additional source of variability in the upwelling process (e.g., Codispoti and Friederich, 1978; Tomczak, 1978).

The present paper describes an investigation of the interleaving observed during the Upwelling 75 Anglo-German experiment off N.W. Africa. Hydrographic stations within 200 km of the coast and time series records of salinity and temperature obtained from moored current meters provide information on the nature of the water mass variability. The aims of the research were to investigate the relation between the interleaving and the larger scale water mass and current configurations, to determine the principal space and time scales of the interleaving, and to estimate if possible the cross-frontal fluxes.

2. Data

The hydrographic, wind and current meter data set from Upwelling 75, with the exception of the salinities derived from current meter conductivities, has been reported by Brockmann *et al.* (1977). In this paper emphasis is given to observations offshore of the continental shelf along line B near 23N (Fig. 1). During the experiment six hydrographic sections were made with a Plessey 9006 STD system and Bathysonde at the standard positions shown in Figure 1. On the same line, three current meter moorings BCM1, BCM2 and BCM3 were located in 74, 515 and 2075 m respectively. The deeper moorings carried Aanderaa current meters at 75, 165, 290, 365 and 505 m, three of which were equipped with conductivity sensors. Only the 49 m current meter at BCM1 is referred to below. Two 12 hr STD time series (8765 and 8772) were made to 300 m depth adjacent to the deep B-line moorings and a Bathysonde 30 hr time series (3656) to 500 m depth was made at a position midway between the moorings (Fig. 1).

Another two hydrographic sections, line A (300 km north of line B) and line C (150 km south), were sampled on a number of occasions. Moorings ACM3 in 3026 m on line A and CCM2 in 507 m on line C carried current meters at roughly the same levels as BCM2 and BCM3. Four of the CCM2 meters had conductivity sensors.

STD or Bathysonde measurements were obtained to at least 500 m at all stations considered here (except the two shallow time series). The data were calibrated by

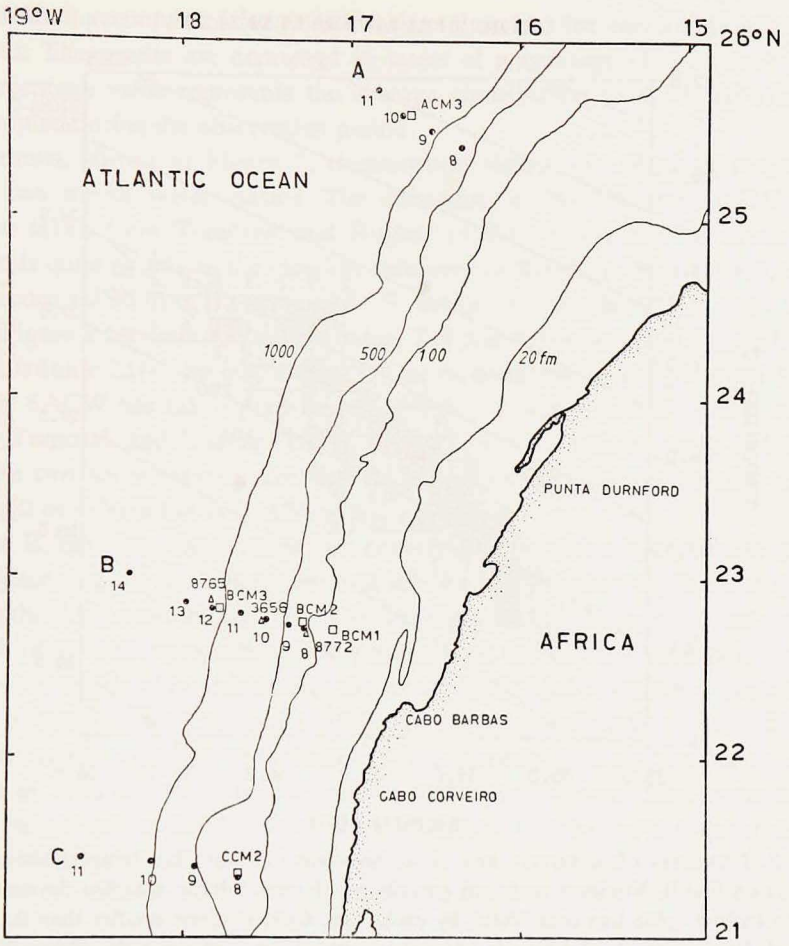

Figure 1. Location of hydrographic stations and current meter moorings during "Upwelling 75": ● standard stations sampled with STD or Bathysonde, △ time series stations, □ current meter moorings. Depth contours are in fathoms (1 fathom = 1.8288 m).

comparison with the results of water bottle casts and were corrected for mismatch of the temperature and conductivity sensor time constants by numerical routines. The current meters recorded at 10 minute intervals throughout the period of hydrographic observations. The current meter temperature and salinity data were compared with nearby hydrographic casts and adjusted where necessary.

3. Water mass characteristics

A frequency of occurrence analysis of the temperature-salinity characteristics on line B was carried out. The method is identical to that of a volumetric census (Mont-

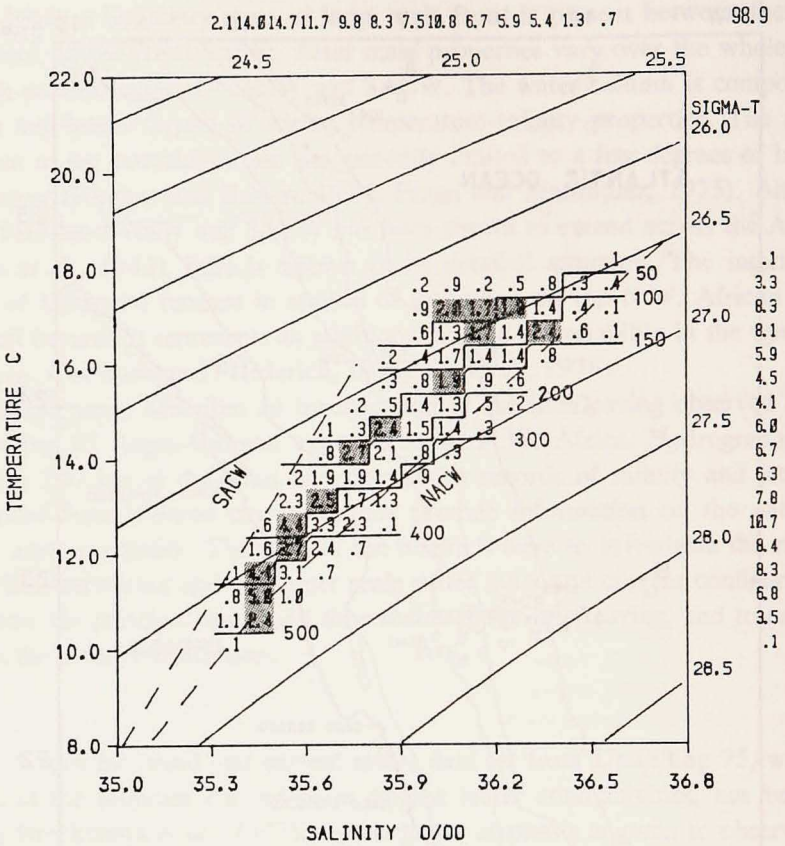

Figure 2. Frequency of occurrence analysis of bivariate and univariate temperature and salinity classes on line B. Numbers represent percentage of total column sampled during repetitions of the hydrographic line contributed by each class. Contributions smaller than 0.1% are excluded. Percentage of total sample volume accounted for is at top right. Heavy lines denote depth contours in meters. The two most common classes in each depth interval are shaded. The shaded area represents 45.9% of the total volume. Lines SACW and NACW indicate the modified forms of the major local water masses.

gomery, 1958), but stations repeated in time rather than spread over an area were utilized. In effect a volumetric census was made for each occupation of line B and then an average census for the whole observation period was obtained. The volume considered was bounded by the sea surface and the 500 m level between the continental shelf edge and 210 km offshore and extended a unit distance alongshore. The temperature-salinity plane was divided into classes 0.5 C $\times$ 0.1‰. Stations were assigned a weight proportional to the distance separating midpoints between the adjacent stations and the time ($\sim$ 5 days, see Fig. 4) between occupations of the station; i.e., each station was assumed typical of a distance along the line and a time between occupations of the line. The weighted temperature-salinity observa-

tions were then accumulated for each bivariate class and the corresponding univariate classes. The results are expressed in terms of percentage of the total volume. Each percentage value represents the average contribution to the total volume of water sampled during the observation period.

The results, shown in Figure 2, demonstrate clearly the effect of interleaving between two source water masses. The definitions of NACW and SACW in the figure are taken from Tomczak and Hughes (1980). While NACW shown here corresponds quite closely to the classical definition of Sverdrup *et al.* (1942), SACW is much more saline than the 'pure' SACW defined by Sverdrup. Since the SACW curve in Figure 2 is based on the least saline *T-S* properties observed during Upwelling 75 at latitude 21N, the implication is that considerable mixing between NACW and 'pure' SACW has taken place south of 21N. However $SACW_{21}$, as it was denoted by Tomczak and Hughes (1980), was a well-defined water mass and formed one of the two source waters involved in the interleaving in the vicinity of 23N. Here, it will be referred to as SACW with no subscript.

On line B, the water mass properties entirely covered the range between the two central water masses. The importance of mixing and interleaving is clear since at many depths the most common *T-S* classes (shaded in Fig. 2) lay near the center of the range of possible properties. The positions of the depth contours in the *T-S* plane were determined by calculating the mean depth of occurrence of each bivariate class as outlined by Carmack (1974). At the isopycnal surface $\sigma_T = 26.6$ the subtropical salinity maximum (Defant, 1961), present in many profiles at depths near 110 m, was evident. The two source water masses were less common than mixtures except below 400 m where the commonest water masses seemed close to unmodified NACW.

4. Analysis of the structure

a. Method. The interaction of the two water masses took the form of numerous inversions of temperature and salinity. An example of an STD profile with significant structure is shown in Figure 3a. In order to quantify the structure, the profiles were separated into "background" and "perturbation" profiles. There are various methods by which this may be achieved, as discussed by Fedorov (1978). Simply subtracting an average B-line profile was precluded by the wide range of *T-S* properties, which would have caused the perturbation profiles to reflect the change from NACW-like to SACW-like properties rather than the variation in amount of structure. The method chosen was to interpolate the profiles to 2 m intervals and to high-pass filter them with a modified binomial weighting scheme like that of Roden (1971). The filter chosen had a cut off wavenumber of 12.5 cycles per kilometer designed to pass all the medium scale structure; i.e., fluctuations of wavelength in the vertical of less than 80 m (and greater than 4 m).

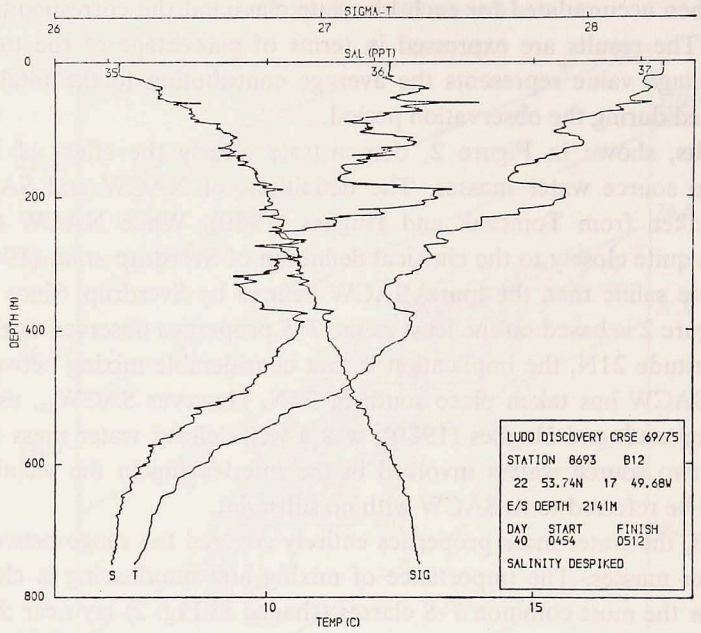

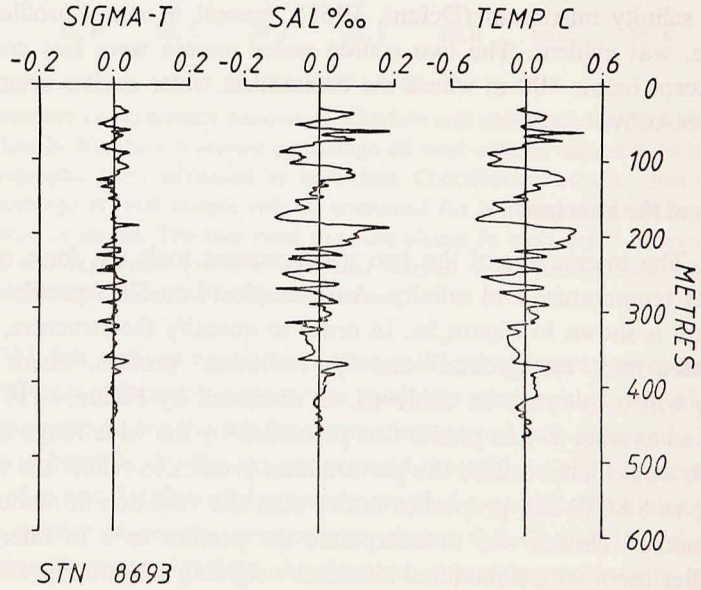

Figure 3. (a) Profiles of temperature (T), salinity (S) and sigma-T (Sig) from a station strongly affected by interleaving; (b) High pass filtered temperature, salinity and sigma-T from the same station. Filter characteristics are given in the text.

The high-passed perturbation profiles (Fig. 3b) faithfully reflected the structure apparent in the original STD profiles and provided a basis for examining the properties of the interleaving as functions of time and space. Mean, standard deviation, skew, kurtosis, extreme values and number of zero crossings were computed over the depth range 0-500 m for all suitable perturbation profiles (0-300 m in the case of the two shallow time series stations). The standard deviation provided a useful index with which to compare the intensity of interleaving in different casts. The lagged cross-correlation coefficient was calculated for each pair of temperature and salinity perturbation profiles. The degrees of freedom pertaining to the calculation were computed by the method of Davis (1976). Finally, as a measure of the overall vertical gradients a least squares linear fit was made to the original profiles.

In the data, the smallest structures were at the Nyquist wavenumber corresponding to the effective sampling interval of 2 m, which is close to the accepted division between medium and small scale structure. Some noise remained at these wavelengths because the despiking correction for time constant mismatch did not eradicate instrumental errors completely. The largest structures occurred at vertical wavelengths close to the cut off of the filter. The boundary between medium and large scale structure is somewhat arbitrary. Although some energy was apparent at wavelengths greater than those passed by the filter, trials showed that inclusion of the longer wavelenghs only marginally affected the results. It is felt that the filtering scheme used here effectively partitions the fields into large scale "background" and medium scale "perturbation" components in the sense described by Joyce (1977).

b. Large scale patterns. Results of the calculations described above, when contoured as a function of time and position along line B, revealed a strong and persistent pattern in the distribution of interleaving (Fig. 4). The most intense structure consistently occurred about 70 km seaward of the shelf-slope break. Both temperature and salinity (Figs. 4a and b) indicated very similar patterns with least interleaving close to the continental slope, an increase of activity to a maximum halfway along the line and then a decrease further seaward. The distribution of structure in the profiles of sigma-T (Fig. 4c) was much more uniform and was uncorrelated with the corresponding temperature and salinity patterns.

As suggested by the similarity of Figures 4a and b, and also by Figure 3b, the temperature and salinity structures were everywhere strongly and positively correlated (Fig. 4d). The highest correlations occurred at zero or infrequently one lag (2 m depth difference). Consequently, there was little effect on interleaving visible in the sigma-T profiles. The temperature perturbations were exactly compensated for their effect on density by the salinity perturbations. The more intense the interleaving was at any location, the higher was the T-S correlation coefficient. However the number of degrees of freedom was high everywhere and so the T-S correlation was always significant at greater than 99% confidence.

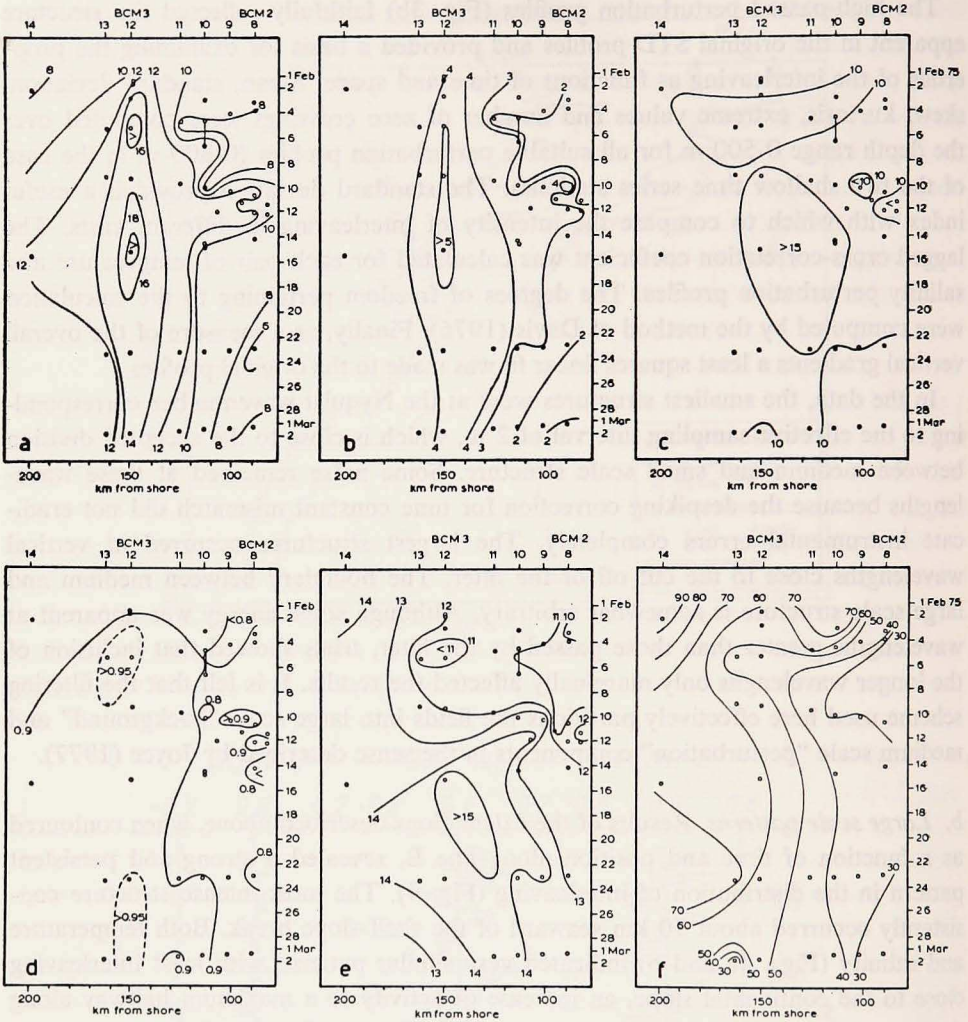

Figure 4. Distance-time contour plots of (a) intensity of temperature structure (standard deviation of high-pass filtered temperature profiles); units are .01 C; (b) intensity of salinity structure—units are .01‰; (c) intensity of sigma-T structure—units are .001 sigma-T; (d) correlation between high-pass filtered temperature and salinity profiles; (e) gradient of linear least squares fit to unfiltered temperature profiles—units are C km^{-1}; (f) depth averaged (0-500 m) percentage contribution of NACW to the water column assuming isopycnal mixing between NACW and SACW as shown in Figure 2.

The statistics of skew and kurtosis indicated that the high-pass filtered records were closest to normality where structure was most intense. Where the intensity was least the structure was frequently dominated by a few isolated features. This was reflected by high values of kurtosis and strong skews of either sign. Elsewhere

the distributions were only slightly peakier than normal and skews on the whole were close to zero. The vertical scale of the structure was given by the number of zero crossings in the high-pass filtered profiles. The average distance between zero crossings for all the stations included in Figure 4 was 25 m for temperature structure and 27.5 m for salinity structure. There was little systematic variation in the number of zero crossings because there was always some weak structure present even in the absence of interleaving. Moreover, interleaved features large in the vertical often had multiple extrema. However, some of the largest amplitude structures were of 30-40 m vertical extent.

There was little evidence to indicate that the intensity of interleaving was related to the vertical gradients. The pattern of variation of the gradient of the linear least squares fit to the temperature profiles (Fig. 4e) was quite different from that of intensity. It was clear, however, that the remarkable pattern in the spatial distribution of interleaving was related to the large scale water mass distribution. At every station, the percentage contribution from both central water masses shown in Figure 2 was calculated at every level, assuming isopycnal mixing. A discussion of the method is given by Tomczak and Hughes (1980). The depth-averaged contribution of NACW was contoured to show its variation in time and with distance offshore (Fig. 4f). The greatest intensity of interleaving occurred where both water masses contributed more or less equally to the water column. Inshore of the interleaving maximum SACW was dominant while to seaward northern water was dominant.

c. Short term variability. The three time series stations allow the importance of shorter time scales to be assessed. This is desirable since the relatively long intervals between line occupations might have resulted in serious aliasing if short term changes were strong. The variability at the time series stations is summarized in Figure 5. The standard deviations of temperature, salinity and sigma-T perturbation profiles and the temperature-salinity correlation coefficient are plotted as a function of time at each position. The scales have been chosen, as in Figure 3b, to approximately reflect the relative importance of temperature and salinity changes on sigma-T in the ranges of interest. Points of general note are the similarity of the variability in temperature and salinity, which is much stronger than in sigma-T, and the persistently high correlation coefficient.

Direct comparison of the three series is complicated by two series extending to only 300 m depth. This has the effect of increasing the value of the standard deviations since in general structure was stronger above 300 m than below (e.g., see Fig. 3b). Inspection of results obtained by utilizing only the upper 300 m at other stations indicates the increase was roughly 25%. Accepting this value, it is seen that the series averaged standard deviations of high-passed temperature and salinity increased from station 8772 nearshore to station 8765 offshore, in accord with the distributions in Figures 4a and b. Changes in the index at the two near-to-shore

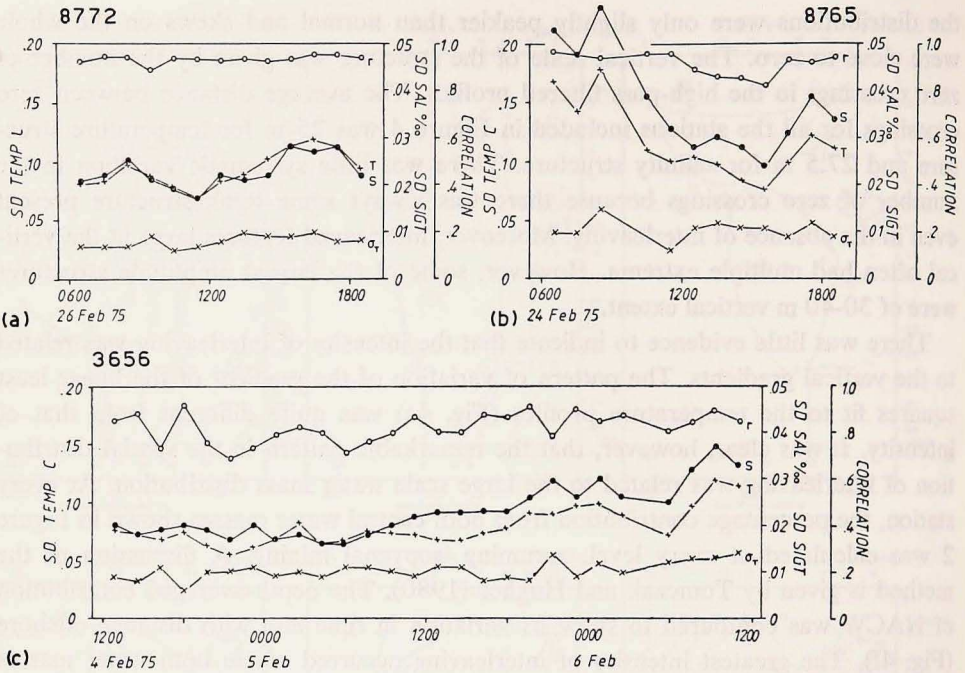

Figure 5. Temporal variation of intensity of temperature (T), salinity (S) and sigma-T (σ_T) structure and correlation (r) of temperature and salinity structure at (a) station 8772 (0-300 m) (b) station 8765 (0-300 m) and (c) station 3656 (0-500 m). See text for explanation.

stations (3656 and 8772) were gradual and small, but at 8765 the index dropped sharply soon after the start of the observations. Inspection of the individual records showed that much of the variance in the first three filtered profiles was contributed by a single feature at the base of the mixed layer. Such pronounced near-surface gradients were rare in the data set. It is considered therefore that the relatively small changes in the remainder of the series at 8765 and at the other two sites were more indicative of the prevailing variability.

The conclusion is that aliasing of the large scale patterns was unlikely. The observation that essentially the same large scale distribution of the interleaving index resulted from every occupation of line B, irrespective of the time of day when it took place, which ship carried out the sampling, or the order in which the stations were sampled would support this conclusion. Furthermore, the temperature and salinity records from moored sensors, discussed below, provided further evidence that the large scale patterns were significant.

5. Variability at the moorings

The current meters equipped with conductivity and temperature sensors provide

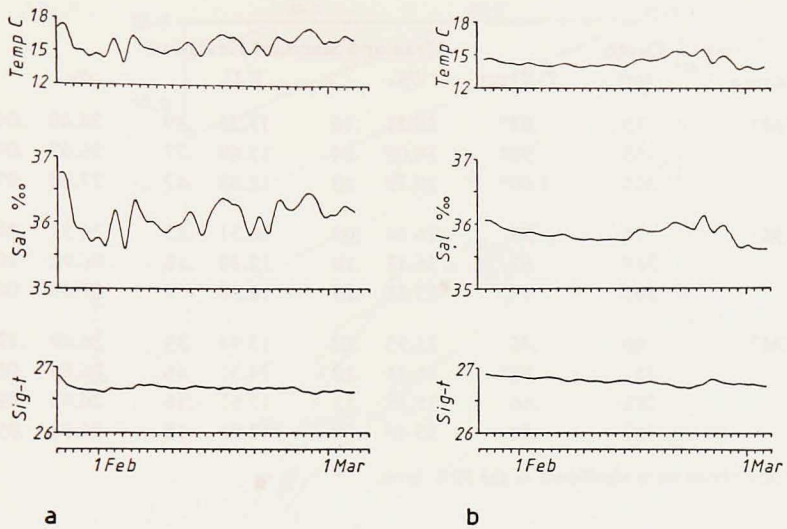

Figure 6. Low-pass filtered time series plots of temperature, salinity and sigma-*T* from moored current meters at (a) 165 m at BCM3 and (b) 157 m at CCM2.

an independent means of examining the *T-S* variability. The two moorings on the hydrographic line each carried three meters so equipped. At BCM3, the position of the interleaving maximum, conductivity records were obtained at 75, 165 and 365 m depth while at BCM2, near the shelf break, records were obtained at 75, 365 and 505 m depth. Another mooring, CCM2, in the same depth as BCM2 (515 m) but about 150 km farther south furnished four more conductivity records at 60, 157, 282 and 357 m depths.

Few observations of salinity from moored sensors have been reported. This is mainly because of problems associated with the cumulative effects of pressure and fouling on the conductivity cells, although Huyer *et al.* (1979) successfully utilized observations off the Oregon coast to examine hydrographic changes during the spring onset of upwelling. The data series considered here contained systematic changes which appear to be partly instrumental in nature. Because of the limited number of STD or Bathysonde observations close enough to the moorings to be useful as a check on the current meter salinities, it was possible only to adjust each series by an additive constant. For this reason, strong but spurious trends remain in some of the salinity records. The original 10 minute series were filtered and decimated to 4 hourly intervals to eliminate all periods less than 40 hours. The analysis was based on the low-pass filtered records because subtidal variability was dominant in the observations in the interleaving zone (Brockmann *et al.*, 1977).

At BCM3, the offshore mooring (Fig. 6a), large changes, up to 0.5‰ and 2°C, occurred over periods as short as one day. In all the records the temperature and

Table 1.

Mooring	Depth (m)	*T-S* corr	Mean and Standard Deviation *S‰*		*T* C		σ_T	
BCM3	75	.93*	36.21	.16	17.26	.49	26.40	.04
	165	.98*	36.09	.24	15.69	.77	26.67	.04
	365	1.00*	35.72	.12	12.88	.47	27.00	.01
BCM2	75	.38	26.14	.09	16.31	.23	26.57	.07
	365	.62	35.47	.14	12.30	.10	26.92	.10
	505	.38	35.35	.05	10.88	.19	27.09	.04
CCM2	60	.45	35.93	.17	15.94	.33	26.49	.12
	157	.86*	35.85	.12	14.31	.46	26.80	.05
	282	.46	35.58	.13	12.67	.16	26.93	.09
	357	.59	35.49	.08	12.06	.15	26.98	.05

Starred correlations were significant at the 99% level.

salinity fluctuations were highly correlated. Consequently little change was evident in the sigma-*T* series. At 365 m on this mooring, below the level of intense interleaving, the amplitude of the fluctuations was reduced and there were fewer changes evident in the record. The complete lack of correlation between fluctuations at different levels indicates that the changes were due to interleaved structures, whose depth scale was shown earlier to be at most less than half the current meter separations.

The salinity records from the moorings closer to shore were more strongly contaminated by drift than the BCM3 records. The 157 m record at CCM2 (Fig. 6b) was the only one which demonstrated fluctuations similar to those seen offshore. The *T-S* correlation was not as high and changes of sigma-*T* occurred through the series. A summary of the temperature, salinity and sigma-*T* records is provided in Table 1. The standard deviations of the temperature records indicate the same increase of interleaving activity offshore as the STD analysis described above. There is less difference in the standard deviations of salinity and sigma-*T* because the instrumental drifts contribute much of the variance in the nearshore records. The *T-S* correlations were much lower at the two nearer-to-shore moorings.

A typical time scale for the fluctuations seen at BCM3 was two days to a week. Taking the record at 165 m as representative of the zone of maximum interleaving, the current observations at that level show a representative mean speed of about 12 cm s^{-1}. Making the assumption that the fluctuations of temperature and salinity seen in Figure 6a were caused by the advection of water parcels past the mooring, then the typical horizontal extent of a parcel would lie between 20 km and 70 km.

The low-pass filtered temperature and salinity data were plotted in the *T-S* plane, grouped by mooring (Fig. 7). The difference in the nature of the recorded *T-S* vari-

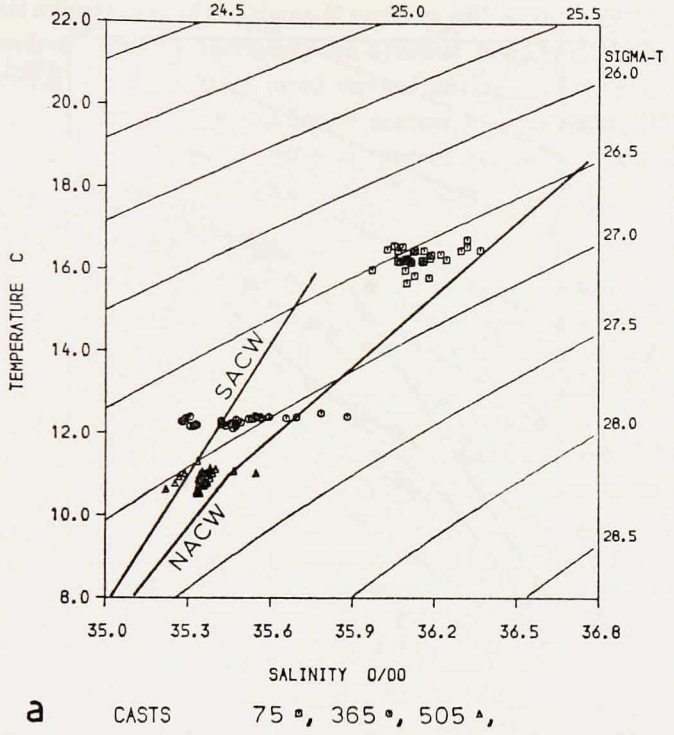

Figure 7. Low-pass filtered salinity and temperature time series from moored current meters plotted in the *T-S* plane at moorings (a) BCM2, (b) BCM3 and (c) CCM2. NACW and SACW curves represent the limits of the major local water masses. Points are plotted at 1 day intervals.

ability offshore and over the inner slope is immediately clear. At BCM3, situated in the maximum of interleaving intensity seen in Figure 4, the low frequency variation was strikingly aligned along surfaces of constant sigma-*T*, emphasizing the importance of lateral mixing. Nearer to shore at BCM2 and CCM2, the *T-S* traces crossed the isopycnal surfaces. A few data points lie well beyond the limits of the NACW and SACW *T-S* curves. These most probably erroneous values represent the ends of the series affected by the drift in salinity. There was little variation of temperature in those series, despite the large changes in salinity. If most of the salinity drift was, as is suspected, instrumental, then the *T-S* curves would be restricted to a much narrower range of sigma-*T* values. The major difference between the offshore and inner slope *T-S* curves would be the range of the *T-S* fluctuations. However, there is insufficient information to confirm this and, certainly, greater variation in sigma-*T* at any depth is to be expected over the inner slope. Changes in the upper levels can occur as a result of upwelling events (Barton *et al.*, 1977)

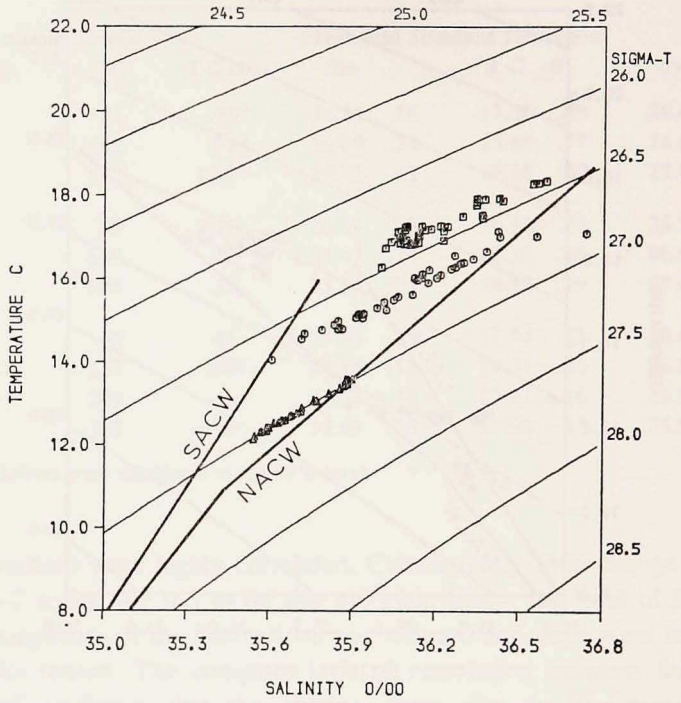

b CASTS 75 ▫, 165 ◦, 365 ▲,

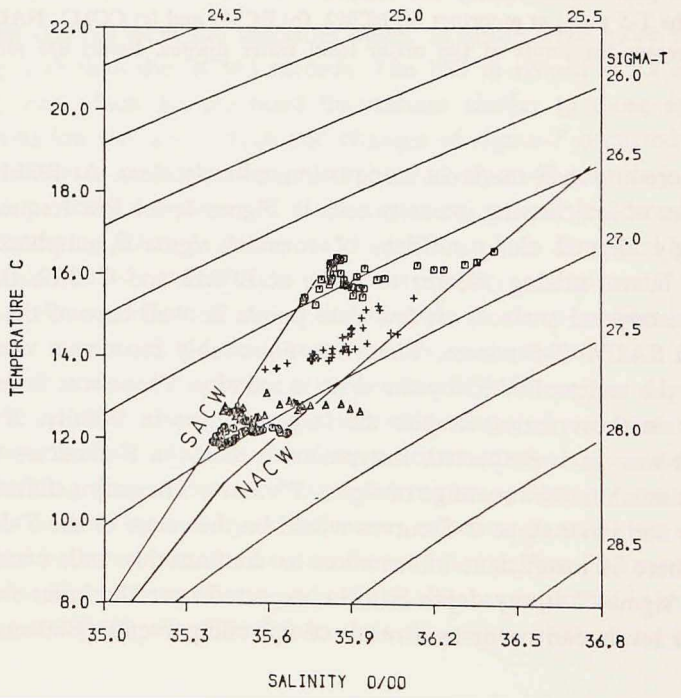

and geostrophic adjustments of the sigma-T surfaces will occur in relation to changes in the slope undercurrent. Furthermore, the dynamic stability over the inner slope may be low enough to result in enhanced vertical mixing (Barton *et al.*, 1982). Interpretation of these T-S data in a different context by Tomczak (1981a) led him to similar conclusions, which were further supported by results of a multiparameter analysis of mixing processes during Upwelling 75 (Tomczak, 1981b).

6. Alongshore variation

The two less frequently sampled hydrographic lines provided valuable information on the alongshore configuration of the interleaving zone. Composite T-S diagrams utilizing casts from each line (Fig. 8) demonstrate the contrasting hydrography of the two lines, roughly 21N and 25N. In the north, T-S characteristics were much more uniform and typical of NACW (Fig. 8a). A weak influence of lower salinity SACW was discernible near 300 m ($\sigma_T = 26.8$) at the stations close to the shelf edge, indicative of poleward flow in the slope undercurrent.

The southern section revealed the presence of both NACW and SACW (Fig. 8b); i.e., T-S properties coincided with the range found on line B. It was evident, however, that although the range was the same, most T-S points on line C lay close to the two source water masses. There was a distinct lack of intermediate values. Stations within about 40 km of the shelf edge possessed SACW-like properties while those farther offshore were close to NACW. Traces of the anomalous Banc d'Arguin water may have been present at two stations on line C (Tomczak, 1981b), but they were impossible to detect with temperature and salinity only and in any case were too weak to have a discernible effect on the present results.

It is clear that much less interleaving was observed on line C than on line B although both source water masses were present. The boundary between NACW and SACW seemed better defined on line C, as may be seen in the vertical sections of Figures 14 and 18 of Tomczak and Hughes (1980). Although stations on either side of the boundary were only 20 km apart, it seems possible that the region of strong interleaving escaped observation during both C-line surveys.

An idealized sketch of the overall situation deduced from the hydrographic and velocity data is presented in Figure 9. A tongue of northward penetrating SACW extended along the continental slope to at least 23N. Mixing with NACW across the offshore boundary of the tongue resulted in a gradual northward dilution until at 25N only a trace of SACW was detectable over the inner continental slope. Mixing at the boundary took the form of interleaving between the two water masses, probably aided by the horizontal shear between the poleward flow of the SACW and the weak equatorward drift of the NACW in the Canary Current. Interleaving petered out toward the north as the difference between the T-S properties of the northward flow and the Canary Current water became less distinct because of horizontal mixing.

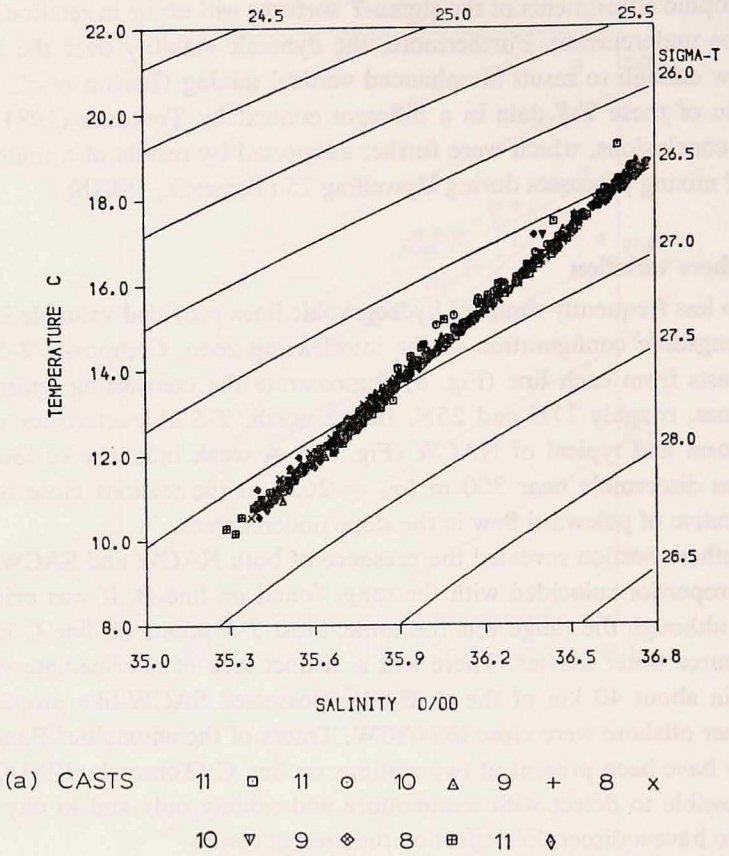

Figure 8. Composite *T-S* plots for hydrographic stations on (a) line A and (b) line C. The cast numbers refer to the standard positions shown in Figure 1.

These ideas are supported by the current observations. Tomczak and Hughes (1980) have discussed the low frequency current variations in some detail, and so only brief reference to them will be made here. Progressive vector diagrams of currents at one intermediate level on each mooring are superimposed on Figure 9. Strong poleward flow over the inner slope was clearly evident at sites CCM2 and BCM2. At both sites the mean flow at all levels was poleward. The shallowest meters on these moorings were at about 75 m, and it was likely that the surface flow was generally equatorward as was reported during JOINT-1 (Mittelstaedt *et al.*, 1975). At 165 m at BCM3 in the center of the interleaving zone, the currents were very variable with virtually no mean alongshore component, perhaps reflecting eddying and meandering associated with interleaving. The other levels at BCM3 indicated similar variability decreasing with depth. Apparently only one mooring, ACM3, was located in the Canary Current. The mean flow at this site was southwestward

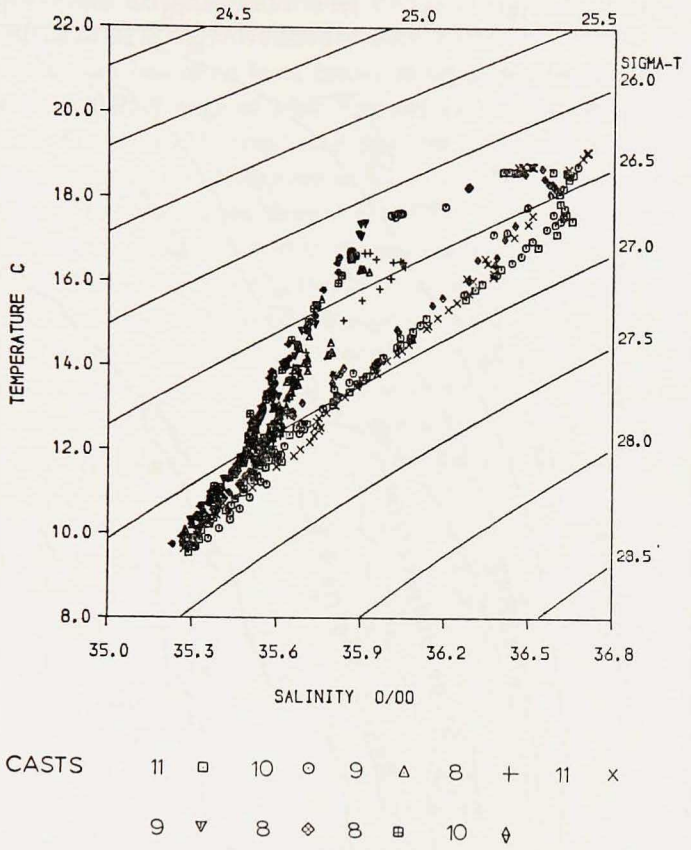

as expected but the observations were dominated by an almost uniform counter-clockwise rotation at all levels in the upper 500 m. This rotation has been interpreted as evidence of a geostrophic eddy with period longer than 30 days (Tomczak and Hughes, 1980).

The last mooring of interest here, BCM1, was on the continental shelf. At this site the flow was strongly equatorward and representative of the coastal upwelling regime, which is dominated by local wind forcing. Considerable interaction between the slope and shelf regimes occurs because upwelling introduces slope waters from depths as great as 200 m onto the shelf (Johnson *et al.*, 1976). This could aid in the dissipation of the anomalous tongue of SACW since water upwelled onto the shelf would be mixed with shelf water and transported southward before being returned to the offshore regime.

7. Discussion

Observations of medium scale interleaved structures in many areas have been

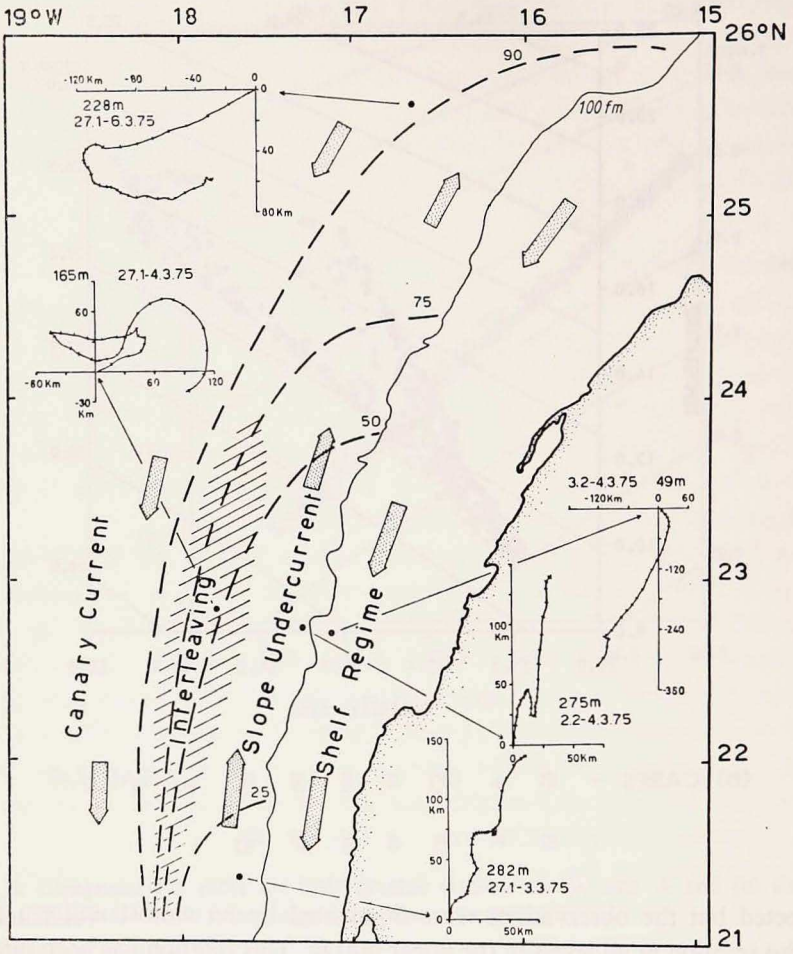

Figure 9. Idealized interpretation of the situation during "Upwelling 75." The heavy broken lines represent the depth averaged (0-500 m) percentage contribution of NACW to the water column. Broad arrows indicate the prevailing currents in the upper 500 m (or the entire water column on the continental shelf). The shaded area represents the zone of interleaving. Progressive vector diagrams of actual currents observed during Upwelling 75 are shown. Marks on the pseudo-trajectories indicate midnight. Start and finish dates are shown.

reported. Interleaving is common at the boundaries of oceanic water masses, such as the Antarctic Polar Front (Gordon *et al.*, 1977) and at the boundaries separating distinct continental shelf and oceanic waters (Coachman and Charnell, 1979). The structures at these boundaries appear horizontally anisotropic. Georgi (1978) found that structures of vertical scale about 100 m extended 3 km parallel to the Antarctic Polar Front and about 1 km across it, while Horne (1978) observed that layers

about 10 m in thickness extended more than 17 km along and several kilometers across the subsurface front in the Nova Scotian slope water.

Intense microstructure has often been found associated with interleaved layers; e.g., on the continental shelf edge of New England (Voorhis *et al.*, 1976). In the California Current, Gregg (1975) concluded that the microstructure was acting to dissipate the intrusions, which in turn were major factors in destroying temperature and salinity features like the saline tongue extending northward along the Baja Californian coast. The situation reported in the present paper seemed similar to that in the California Current. Undoubtedly, the interleaving was acting to dissipate the tongue of SACW intruding poleward across lines C and B, and presumably microstructure was dissipating the interleavings although it could not be resolved with the available instrumentation. Indirect evidence of microscale activity was seen in the form of thermohaline 'steps' beneath the subtropical salinity maximum at one site, and has been reported by Barton *et al.* (1982). Similar but less well-defined steps are seen in Figure 3 below 200 m.

The exchange of water masses across such frontal boundaries implies a horizontal flux of heat and salt. Joyce (1977) proposed a model which allows a rough estimate of the turbulent transfer rate through the frontal zone. The temperature field is assumed separable into three scales—large (overbar), medium (tilde) and small (prime):

$$T = \bar{T} + \tilde{T} + T'$$

where $\overline{\tilde{T}} = \tilde{T}' = 0$. The large scale is considered representative of the water mass variations across fronts, the medium scale of the related interleaving along density surfaces, and the small scale of the dissipative microstructure and associated exchanges. The cross-frontal temperature flux may then be expressed in Joyce's notation as

$$F_T = -\overline{\tilde{v}\,\tilde{T}} = \overline{A_T{}^v \left(\frac{\partial \tilde{T}}{\partial z}\right)^2} \Big/ \frac{\partial \bar{T}}{\partial y}. \tag{1}$$

The flux can also be written

$$F_T = \overline{A}_T{}^H \frac{\partial \bar{T}}{\partial y} \tag{2}$$

where $\overline{A}_T{}^H$ is the horizontal diffusivity. Therefore,

$$\overline{A}_T{}^H = \overline{A_T{}^v \left(\frac{\partial \tilde{T}}{\partial z}\right)^2} \Big/ \left(\frac{\partial \bar{T}}{\partial y}\right)^2 . \tag{3}$$

All the terms on the right-hand side of (1) and (3) can be estimated from vertical profiles except for $A_T{}^v$.

The cross-frontal horizontal temperature gradient term in (1) and (3) was esti-

mated for the upper 500 m from hydrographic sections on line B. Values of the vertical gradient of medium scale temperature term were obtained from the STD profiles filtered as described above. The vertical exchange coefficient A_T^v was assumed equal to a constant value of 1 $cm^2\ s^{-1}$, which falls in the range of values considered by Joyce (1977). Hence F_T, the cross-frontal temperature flux was 1 C cm s^{-1} and the associated horizontal diffusivity has a value of 6×10^6 $cm^2\ s^{-1}$.

A second, independent, estimate of F_T could be made by utilizing directly the observations of temperature and velocity at mooring BCM3 in the center of the interleaving zone. In this case, $\tilde{v}$ and $\tilde{T}$ were taken to be represented by the deviations from the record mean of the low pass filtered cross-frontal (east-west) component of velocity and temperature series. Five records were available in the upper 500 m, each of which furnished an estimate of F_T. The weighted depth mean of these resulted in an overall value of the temperature flux equal to 2 C cm s^{-1}. The corresponding value of the horizontal diffusivity was then 10^7 $cm^2\ s^{-1}$.

Taking the width of the tongue of SACW against the coast to be 50 km from shelf edge to the frontal boundary and considering the average temperature anomaly with respect to the surrounding NACW to be −1 C over the upper 500 m layer, then the heat deficit per centimeter alongshore was 2.5×10^{11} cal. The cross-frontal heat fluxes estimated above would compensate the deficiency in 30-60 days in the absence of advective or other effects. The tongue of SACW was presumably maintained by a rough balance between northward advection and horizontal diffusion although upwelling and recirculation southward on the continental shelf could be important.

The agreement between the two independent estimates of the heat flux was surprisingly good considering the disparate nature of the two data sets involved and the numerous tacit assumptions made in the partition of the temperature field and the equivalence of temporal and spatial means. The values were somewhat larger than those found by Joyce *et al.* (1978) in the Antarctic Polar Front, which is to be expected because of the more intense nature of the interleaving found off N.W. Africa. While large scale changes such as seasonal variation in the position of the tongue might not alter the cross-frontal fluxes at a position fixed relative to the front, the possibility exists that meanderings of the front itself and separation of eddies would dominate cross-frontal transports.

8. Concluding remarks

The above analysis has provided a number of results:

1. The interleaving zone off N.W. Africa has been demonstrated to be intimately associated with a well-defined front between North and South Atlantic Central Water masses. Partitioning of the hydrographic fields into large and medium scale by numerical filtering allowed the spatial and temporal variation of the interleaving

to be quantified. The resulting distribution of interleaving intensity was supported by time series observations at five moorings, which showed that interleaving was occurring along the offshore edge of a northward flowing tongue of SACW over the inner continental slope. During the four week observation period, the situation did not vary significantly.

2. The space and time scales of the interleaved structures which emerged were: vertical scale 25-30 m, horizontal scale 20-70 km parallel to the front and <10 km across the front, time scale 2-7 days. The spatial resolution of the data did not, however, allow definitive estimates of the horizontal scales.

3. Estimates of cross-frontal heat flux, made using the model of Joyce (1977), provided values close to 1 C cm s^{-1}.

The present data set is insufficient to allow a detailed investigation of interleaving processes. Nevertheless, it has provided a clear picture of the relationship of the zone of interleaving to local oceanic conditions. In addition, it has been possible to make preliminary estimates of the dominant scales and horizontal fluxes. An improvement in the estimates of these requires better horizontal and vertical resolution. Identification and evaluation of the importance of small scale processes, such as cross isopycnal movement of intrusions (Gregg, 1980; Stern, 1967), can only be attained by detailed and repeated fine scale measurements.

Acknowledgments. "Upwelling 75" was a co-operative field program between the University of Liverpool and the Institut for Meereskunde, Kiel, supported by the Natural Environment Research Council of Great Britain and the Deutsche Forschungsgemeinschaft, F. R. G. This research was supported financially by N.E.R.C. grant GR3/3522.

REFERENCES

Barton, E. D., P. Hughes and J. H. Simpson. 1982. Vertical shear observed at contrasting sites over the continental slope off N.W. Africa. Oceanologica Acta, *5*, 169–178.

Barton, E. D., A. Huyer and R. L. Smith. 1977. Temporal variation observed in the hydrographic regime near Cabo Corveiro in the northwest African upwelling region, February to April 1974. Deep-Sea Res., *24*, 7–23.

Brockmann, C., P. Hughes and M. Tomczak. 1977. Currents, winds and stratification in the N.W. African upwelling region during early 1975. Data Report 32, Institut fur Meereskunde an der Christian-Albrechts-Universitat, Kiel, 45 pp.

Carmack, E. 1974. A quantitative characterization of water masses in the Weddell Sea during summer. Deep-Sea Res., *21*, 431–442.

Coachman, L. K. and R. L. Charnell. 1979. On lateral water mass interaction—a case study, Bristol Bay, Alaska. J. Phys. Oceanogr., *9*, 278–297.

Codispoti, L. A. and G .E. Friederich. 1978. Local and mesoscale influences on nutrient variability in the northwest African upwelling region near Cabo Corveiro. Deep-Sea Res., *25*, 751–770.

Davis, R. E. 1976. Predictability of sea surface temperature and sea level pressure anomalies over the North Pacific Ocean. J. Phys. Oceanogr., *6*, 249–266.

Defant, A. 1961. Physical Oceanography, Volume 1. Pergamon Press, London, 729 pp.

Fedorov, K. N. 1978. The thermohaline finestructure of the Ocean. Pergamon Press, London, 170 pp.

Fraga, F. and M. Manriquez. 1975. Oceanografía química de la región de afloramiento del noroeste de Africa. II. Campaña "Atlor II", marzo 1973. Resultados expediciones científicas del buque oceanográfico "Cornide de Saavedra", *4,* 185–218.

Georgi, D. T. 1978. Finestructure in the Antarctic Polar Front Zone. Its characteristics and possible relationship to internal waves. J. Geophys. Res., *83,* 4579–4588.

Gordon, A. L., D. T. Georgi and H. W. Taylor. 1977. Antarctic Polar Front Zone in the Western Scotia Sea—Summer 1975. J. Phys. Oceanogr., *7,* 309–328.

Gregg, M. C. 1975. Microstructure and intrusions in the California Current. J. Phys. Oceanogr., *5,* 253–278.

—— 1980. Three dimensional mapping of a small thermohaline intrusion. J. Phys. Oceanogr., *10,* 1468–1492.

Horne, E. P. W. 1978. Interleaving at the subsurface front in the slope water off Nova Scotia. J. Geophys. Res., *83,* 3659–3671.

Hughes, P. and E. D. Barton. 1974. Stratification and water mass structure in the upwelling area off northwest Africa in April/May 1969. Deep-Sea Res., *21,* 611–628.

Huyer, A., E. J. C. Sobey and R. L. Smith. 1979. The spring transition in currents over the Oregon continental shelf. J. Geophys. Res., *84,* C11, 6995–7011.

Johnson, D. R., E. D. Barton, P. Hughes and C. N. K. Mooers. 1976. Circulation in the Canary Current off Cabo Bojador in August 1972. Deep-Sea Res., *22,* 547–558.

Joyce, T. M. 1977. A note on the lateral mixing of water masses. J. Phys. Oceanogr., *7,* 626–629.

Joyce, T. M., W. Zenk and J. Toole. 1978. The anatomy of the Antarctic Polar Front in the Drake Passage. J. Geophys. Res., *83,* C12, 6093–6113.

Mittelstaedt, E., R. D. Pillsbury and R. L. Smith. 1975. Flow patterns in the Northwest African upwelling area. Dt. Hydrogr. Z., *28,* 145–167.

Montgomery, R. B. 1958. Water characteristics of Atlantic Ocean and of world ocean. Deep-Sea Res., *5,* 134–148.

Roden, G. I. 1971. Spectra of North Pacific temperature and salinity perturbations in the depth domain. J. Phys. Oceanogr., *1,* 25–33.

Stern, M. E. 1967. Lateral mixing of water masses. Deep-Sea Res., *14,* 747–753.

Sverdrup, H. U., M. W. Johnson and R. H. Fleming. 1942. The Oceans: Their Physics, Chemistry and General Biology. Prentice-Hall, Engelwood Cliffs, 1087 pp.

Tomczak, M. 1978. De l'origine et la distribution de l'eau remontee a la surface au large de la cote Nord-Ouest Africaine, Ann. Hydrogr. Ser. 5, *6,* 5–14.

—— 1981a. Longshore advection during an upwelling event in the Canary Current area as detected by airborne radiation thermometer. Oceanologica Acta, *4,* 161–169.

—— 1981b. An analysis of mixing in the frontal zone of South and North Atlantic Central Water off Northwest Africa. Prog. in Oceanogr., *10,* 173–192.

Tomczak, M. and P. Hughes. 1980. Three-dimensional variability of water masses and currents in the Canary Current upwelling region. "Meteor" Forsch.-Ergebnisse Reihe A, *21,* 1–24.

Voorhis, A. D., D. C. Webb and R. C. Millard. 1976. Current structure and mixing in the shelf/slope water front south of New England. J. Geophys. Res., *81,* 3695–3708.

Received: *27 October, 1981;* revised: *25 June, 1982.*